Earth Surface Processes and Landforms
Earth Surf. Process. Landforms **24**, 423–435 (1999)

SAND TRANSPORT AND DEPOSITION WITHIN ARRAYS OF NON-ERODIBLE CYLINDRICAL ELEMENTS

JASEM M. AL-AWADHI[1]* AND BRIAN B. WILLETTS[2]

[1]*Environmental and Earth Science Division, Kuwait Institute for Scientific Research, PO Box 24885, 13109 Safat, Kuwait*
[2]*Deparment of Engineering, University of Aberdeen, Fraser Building, Kings College, Aberdeen AB9 2UE, UK*

Received 6 July 1998; Revised 7 September 1998; Accepted 10 September 1998

ABSTRACT

The study concerns sand deposition within a regular array of vertical cylinders placed in the path of a sand-laden wind. Twelve wind tunnel experiments using three preselected shear velocities (28·78, 32·86 and 45·1 cm s^{-1}), with associated rates of sand feed (0·3, 2·0 and 3·8 g cm^{-1} s^{-1}), and four roughness element concentrations (λ = 0·046, 0·092, 0·184 and 0·369) were carried out to evaluate the factors that affect sand deposition and sand flux in the presence of immobile rough elements. The measurements showed that as the concentration of non-erodible elements increased, the percentage reduction in the initial sand flux increased and a particularly sharp reduction occurred when $\lambda \geq 0{\cdot}18$. The pattern of reduction was found to be $q_{red} = q_{eq}\ (d/H)\ [\Delta y/(\Delta y - d)](0{\cdot}68\ -3{\cdot}5\lambda)$ when $\lambda \leq 0{\cdot}18$, and $q_{red} = q_{eq}(d/H)[\Delta y/(\Delta y - d)](0{\cdot}025)$ when $\lambda > 0{\cdot}18$, where q_{eq} is the equilibrium rate of sand transport arriving at the best bed, d is the diameter of the cylinder, H is the height of the cylinder, and Δy is the width of unit area associated with a cylinder.

The experimenal results also showed that the sand flux downstream of the array started to increase immediately upon the commencement of burial of the array's cylinders. Thus the sand deposition and sand flux along an array consisting of regularly distributed, non-erodible elements were shown to be neither uniform nor steady. Copyright © 1999 John Wiley & Sons, Ltd.

KEY WORDS: wind tunnel; sand flux; deposition; non-erodible element

INTRODUCTION

The literature relating to flow over rough elements of various kinds is concerned with two principal features. The first is the development of a boundary layer appropriate to the rough surface and the influence of roughness in inducing transition (e.g. O'Loughlin and Macdonald, 1964; Bradley, 1968; Antonia and Luxton, 1971; Jensen, 1978). The second feature that is widely studied concerns the drag caused by non-erodible elements in a fully developed turbulent shear flow (e.g. Marshall, 1971; Wooding *et al.*, 1973; Lyles and Allison, 1975; Arya, 1975). Several studies focus on the reduction that non-erodible elements produce in boundary shear stress on the surface between them and the consequent influence on the threshold of sand particle movement (e.g. Gillette and Stockton, 1989; Boundy and Leach, 1990; Nickling and McKenna Neuman, 1995). Table I reviews the aims and the roughness-element configurations of some experimental studies.

It is the purpose of this study to explore some aspects of the effect of non-erodible elements on sand transport rate and sand deposition. Attention is focused on the upwind boundary of an array of regularly spaced cylinders of equal height so as to examine the deposition when a sand-laden wind first encounters a pattern of fixed roughness. The influence on deposition in this zone of cylinder dimensions and spacing was measured in a series of 12 wind tunnel experiments. The paper reports the experiments and discusses the observed spatial and temporal gradients of deposition rate in terms of concentration λ, the ratio of silhouette area to floor area per element (Marshall, 1971). The ratio of transport rate escaping the 250 cm long array to

* Correspondence to: Dr J. M. Al-Awadhi, Environmental and Earth Science Division, Kuwait Institute for Scientific Research, PO Box 24885, 13109 Safat, Kuwait. Email: jawadhi@kisr.edu.kw

CCC 0197-9337/99/050423–13 $17.50

Table I. Summary of some experimental non-erodible element studies

Roughness element	H (cm)	H/d	$1/\lambda$	Reference	Purpose
Spheres Spherical segments Truncated cones Transverse short strip	0·41, 0·21 0·26 0·375 0·3	1 0·325 0·47 0·375	6–95 19–77 13–53 16–67	Schlichting (1936)	Measurements of total drag for each configuration at different Reynolds number.
Cubes	0·475	1	64–256	O'Loughlin and Macdonald (1964)	Investigating overall resistance in channel flow containing concentration cubes and natural sand grains.
Cylinders Hemispheres	2·54 2·54	0·2–2 0·5	18–1250 18–1250	Marshall (1971)	Investigating the effect of different size and distribution of the rough elements on total shear and on partition of stress.
Cylinders Spheres	3·81 2·434	5·81 – 2·39 1	2·5–35 4·8 and 19·22	Lyles *et al*. (1974)	To determine the critical surface barrier ratio for different wind speeds.
Sphere	0·24 0·43 1·12	1 1 1	Packed closely	Gillette and Stockton (1989)	Same as Lyles *et al*. (1974) but with different set-up of the rough elements in a different wind tunnel.
Rectangular prism Cylinders	8 10 5 0·6 1 8·5	0·5 1, 0·66 1 0·16, 0·14, 0·1 1 0·66	Single N/A	Iversen *et al*. (1991)	Determine the effect of such boundary layer obstacles on local aeolian saltation erosion and deposition.
Cylinders	N/A	d = 0·66 and 1·59 (cm)	11–387 element per m^2	Lyles and Allison (1975)	Studying the effect of uniformly spacing non-erodible elements on wind direction variability.
Blocks (3·8 cm wide and 1·9 cm thick)	5·7		10·74	Boundy and Leach (1990)	Examining how surface roughness in the form of regularly spaced blocks affects the threshold velocity and flux of fine sand at both Earth and Mars surface pressure.
Spheres	1·64	1	7·4 and 4·74	Al-Sudairawi (1992)	Determining the specifications of the rough elements at which the sand transport ceased.
Spheres	1·8	1	1·1, 3·06 and 12·25	Nickling and McKenna Neuman (1995)	Measuring the transport of erodible particles, well-sorted fine sand, with time over three different beds.

λ Concentration of non-erodible element, equal to frontal area divided by floor area; H, height of non-erodible element; d, maximum frontal width of non-erodible element.

the rate upwind is also reported. The escape (or penetration) rate is of particular significance in the design of practical sand control measures.

THE EFFECT OF NON-ERODIBLE ROUGHNESS ON SAND TRANSPORT AND DEPOSITION

The effect of large surface roughness elements on the sand transport phenomenon can be discussed in terms of three main points.

Firstly, the non-erodible elements reduce the shear stress on the erodible surface. As roughness increases, although total boundary shear stress increases, a greater percentage is taken up by the non-erodible elements,

leaving less stress on the intervening surface to move the erodible sand particles (Marshall, 1971; Lyles *et al.*, 1974; Lyles, 1977). Thus, the number of grains directly entrained by the fluid is reduced. Gillette and Stockton (1989) and Nickling and McKenna Neuman (1995) have suggested that shear stress on the intervening sand surface goes to zero when $\lambda \cong 0{\cdot}5$, resulting in a cessation of sediment transport.

Secondly, in low-density arrays, non-erodible elements tend to increase the local dislodgment rate in some places owing to the development of near-bed turbulent eddies (Logie, 1982). Nickling and McKenna Neuman (1995), using four different spacings, D, of glass marbles, each exposed to two preselected free-stream velocities (8 and 10 m s^{-1}), confirmed this. They found that the sand transport rate was enhanced in the presence of non-erodible elements over a limited range of concentration (e.g. $\lambda = 0{\cdot}04$–$0{\cdot}06$, $0{\cdot}016$–$0{\cdot}025$, $0{\cdot}006$ and $0{\cdot}0015$ for $D = 1{\cdot}8$, 3, 6 and 12 cm, respectively), but that with increasing concentration beyond this range the sand transport rate decays rapidly. They attribute this enhancement in the sand flux to two factors: (i) an increase in shear velocity due to the increase in surface roughness; and (ii) an increase in the number of highly elastic collisions between saltating grains and the roughness elements, promoting grain ejection and transport.

Thirdly, the non-erodible elements directly reduce the number and effect of grain/bed collisions on the erodible surface. Al-Sudairawi (1992) stated that non-erodible elements shelter a portion of the erodible surface, preventing saltating grains from impacting and splashing up new grains. He noted that sheltering, which can be viewed as a shadow downwind of the non-erodible elements, is a function of the approach angle of the saltating grains (9–14°) and the aspect area of the elements.

Although some predictive formulae for equilibrium sand flux over non-erodible elements are found in the literature (e.g. Ash and Wasson, 1983; Buckley, 1987), there is no reliable method of predicting sand transport change with time or element density in these circumstances (McKenna Neuman and Nickling, 1995). Mathematically, sand will be deposited around non-erodible elements if $\partial q/\partial x$ is less than zero, where q is the rate of sand transport per unit time per unit width. The net rate at which sand is deposited in each unit area associated with an element is $(q_s - q_o)$ where q_s is the rate at which sand is being supplied immediately upwind of the area, and q_o is the rate immediately downwind. Thus over any period, Δt, the weight of net deposition is $(q_s - q_o)\,\Delta t$, and the volume change of sand present in the unit area is $(q_s - q_o)\Delta t/\gamma$, where γ is the bulk specific weight of the sediment.

The local increase in the average height of sand accumulation on the non-erodible element, z, can then be calculated from the sediment continuity equation:

$$y\partial z/\partial t + 1/\gamma(\partial q/\partial x) = 0 \tag{1}$$

where y is the width of the associated area normal to the wind.

Equation 1 can be re-expressed in finite difference form as:

$$\Delta z = (q_s - q_o)\Delta t/(\gamma \Delta y \Delta x) \tag{2}$$

where Δz is the increment of change of the sand accumulation height in time Δt, and Δy is the width of unit area associated with a non-erodible element.

EXPERIMENTAL SET-UP AND PROCEDURES

The experiments were carried out in a 1200 -cm long wind tunnel with cross-sectional dimensions 50 cm by 50 cm. For the same wind tunnel Al-Sudairawi (1992) found that sand flux increased for approximately 600 cm before reaching equilibrium. Accordingly, the test bed consisting of cylinders was placed with its upwind boundary at 720 cm from the tunnel entrance (Figure 1) so that equilibrium sand flux was established upwind of the bed. Sand was fed by a sand feed system (Al-Awadhi and Willetts, 1998) near the tunnel entrance to maintain the supply of sand available for transport. To develop a fully rough condition quickly, static roughness was created by means of cylinders 1·1 cm in height and 0·9 cm in diameter, evenly and uniformly spaced at a centre-to-centre distance of twice the cylinder diameter for a distance of 150 cm

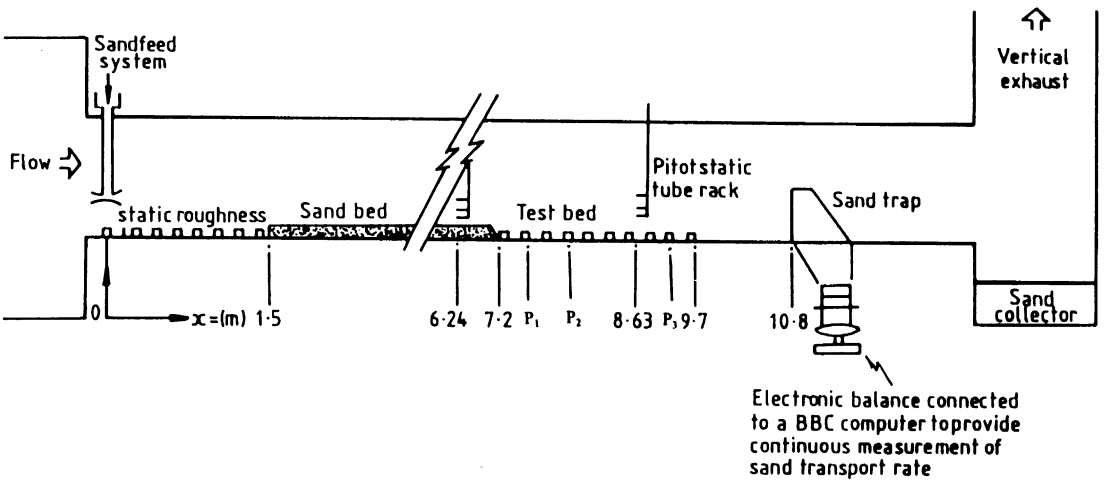

Figure 1. Schematic side elevation of the tunnel showing the positions of the test bed and of instrumentation

Table II. Main experiment specifications and associated measurements

Experiment no.*	Cylinder diameter, d (cm)	Cylinder height, H (cm)	Spacing, D (cm)	Roughness density, λ	Rate of sand feed (g cm^{-1} s^{-1})	u (cm s^{-1})	Height of wind velocity measurements at x = 143·5 cm† (cm)	Run duration (s)
A1-25T	2·3	2·3	9·2	0·046	0·3	28·7	3·1, 4·1, 6·5	1470
A1-30T	2·3	2·3	9·2	0·046	2	32·8	3·1, 4·1, 6·5	1470
A1-40T	2·3	2·3	9·2	0·046	3·8	45·1	3·1, 4·1, 6·5	1470
A2-25T	2·3	4·6	9·2	0·092	0·3	28·7	5·6, 6·6, 9·0	2970
A2-30T	2·3	4·6	9·2	0·092	2	32·8	5·6, 6·6, 9·0	2970
A2-40T	2·3	4·6	9·2	0·092	3·8	45·1	5·6, 6·6, 9·0	2970
A3-25T	2·3	2·3	3·45	0·184	0·3	28·7	3·1, 4·1, 6·5	5070
A3-30T	2·3	2·3	3·45	0·184	2	32·8	3·1, 4·1, 6·5	3600
A3-40T	2·3	2·3	3·45	0·184	3·8	45·1	3·1, 4·1, 6·5	2100
A4-25T	2·3	4·6	3·45	0·369	0·3	28·7	5·6, 6·6, 9·0	2970
A4-30T	2·3	4·6	3·45	0·369	2	32·8	5·6, 6·6, 9·0	2970
A4-40T	2·3	4·6	3·45	0·369	3·8	45·1	5·6, 6·6, 9·0	2970

* A and the following number indicate the array number; T and the preceding number indicate the wind speed based on number of turns of the vane throttle.
† x is a downwind distance measured from the upwind edge of a test bed.

downstream from the position of the sand feed tubes. These measures ensured that the array was fed by a uniform sand flux of the value appropriate to the shear velocity in each experiment. In the reference frame of Figure 1 the array extends from $x = 720$ to $x = 970$ cm.

Twelve main experiments incorporated three preselected shear velocities with associated rates of sand feed and four array densities (test beds). The physical characteristics of the four roughness arrangements and the specifications of the different experiments are presented in Table II. Three types of data were recorded (see Figure 1): (i) the wind profiles upwind, at $x = 624$ cm, and above the test bed at $x = 863$ cm; (ii) the sand flux downwind of the test bed, i.e. at $x = 1080$ cm; and (iii) the depth of sand cover around cylinders at three cross-sections along each test bed as detailed below.

The rate of sand flux escaping the test bed was monitored continuously using a sand trap with inlet width and height of 2 cm and 20 cm, respectively. The trap was 360 cm downwind from the leading edge of the test bed and provided a continuous record of the accumulated weight of transported sand as a function of time.

Periodical estimates of the depth of the deposited sand were obtained photographically. Two cameras were used at each of three positions, namely, P1 = 39·8 cm, P2 = 119·4 cm and P3 = 199 cm downwind from the leading edge (x = 759·8, 839·4 and 919 cm). One of each pair of cameras was installed on the roof of the wind tunnel to monitor the deposition between the cylinders. The other one was installed at the side of the wind

tunnel to record the height of sand accumulation on the cylinders. The deposits were photographed at regular time intervals; the chosen interval in a particular experiment was in the range 60 to 180 s depending on the wind speed and roughness density.

RESULTS

Visual and quantitative observations

Direct observation and video recording indicated that as the sand started to move, a proportion of the saltating grains impacted on the cylinder surfaces and bounced back to continue moving between and above the cylinders. The number of grains so impacting increased with increase in cylinder height, and with increase in cylinder density. Other grains became trapped in the wind shadows of the cylinders (lee-side). The development of lee-side deposition was recorded photographically as a function of time. The photographs showed that this kind of deposit began to form immediately, and quickly finalized its plan shape. Figure 2 shows the formation of the lee-side deposition with time in one particular experiment. The development shown is typical of the range of experiments, although the rate of development differs with experimental conditions.

For the lowest-density arrays (Table II), elements in the upwind row were the first to be buried by sand and these were followed by gradual burial of the downwind rows progressively. For the other array densities, the initial deposition affected not only the front row, but also cylinders in rows further downwind. The floor between the rows continued to accumulate sand until entire rows became covered to a critical height (i.e. to a maximum depth of sand deposition which varied between 0·5 and 1 cm from the top surface of the cylinder, depending on the wind strength and the cylinder density). The cylinders were never totally buried because of local wind scouring. As a result of this a sand accumulation patch with an aerodynamic shape (aerofoil) was a permanent feature downwind of each completely buried cylinder. A concave surface of deposited sand was also formed between adjacent buried cylinders. This concavity is attributable to the non-uniformity in the surface shear stress distribution on the intervening deposited-sand surface and to the distribution of saltation impacts. The detailed superficial topographic features of the deposits of sand around a cylinder were measured using a laser displacement profiler (LDP) technique. The patterns in all cases had similar shapes; an example is presented in Figure 3.

Early in each run, other than at the highest array density, saltating grains were detectable by eye. Some particles were seen to move in creep mode within the wake zone and others in saltation mode between the cylinder wakes.

Burial of the cylinders and sand deposition

The cylinders were gradually buried by sand. The rate at which a particular cylinder was buried varied with the upstream wind strength and the spacing between the cylinders. In most cases, a high rate of sand deposition occurred during the first few minutes after start-up. Good definition of this phase of deposition was achieved only in the experiments with tighter spacing ($D = 3{\cdot}3{\cdot}45$ cm) and shorter height ($H = 2{\cdot}3$ cm), i.e. array A3. Figure 4 illustrates the change of the exposed heights of the cylinders in three experiments with array A3 ($\lambda = 0{\cdot}184$). The exposed height is equal to the distance from the top surface of the cylinders down to the sand lying immediately downwind of the cylinder centre. The change is shown at each of three predetermined positions, P1, P2 and P3 (Figure 1). Sand height was estimated from photographs of a vertical scale marked on the cylinder. Figure 4 shows that the cylinders along the test bed were not buried synchronously. They remained partially clear of sand for some time, after which they began to be buried progressively at a rate depending on the wind strength. The onset and rate of burial were a function of the position of the monitored cylinder in the array. The onset of burial was earlier for cylinders near the upstream edge of the array and their rate of burial was quicker.

The relationship between the escaping sand flux measured by the sand trap and the exposed height of the cylinders at the chosen positions in array A3 was studied and it was found that sand flux increased as the

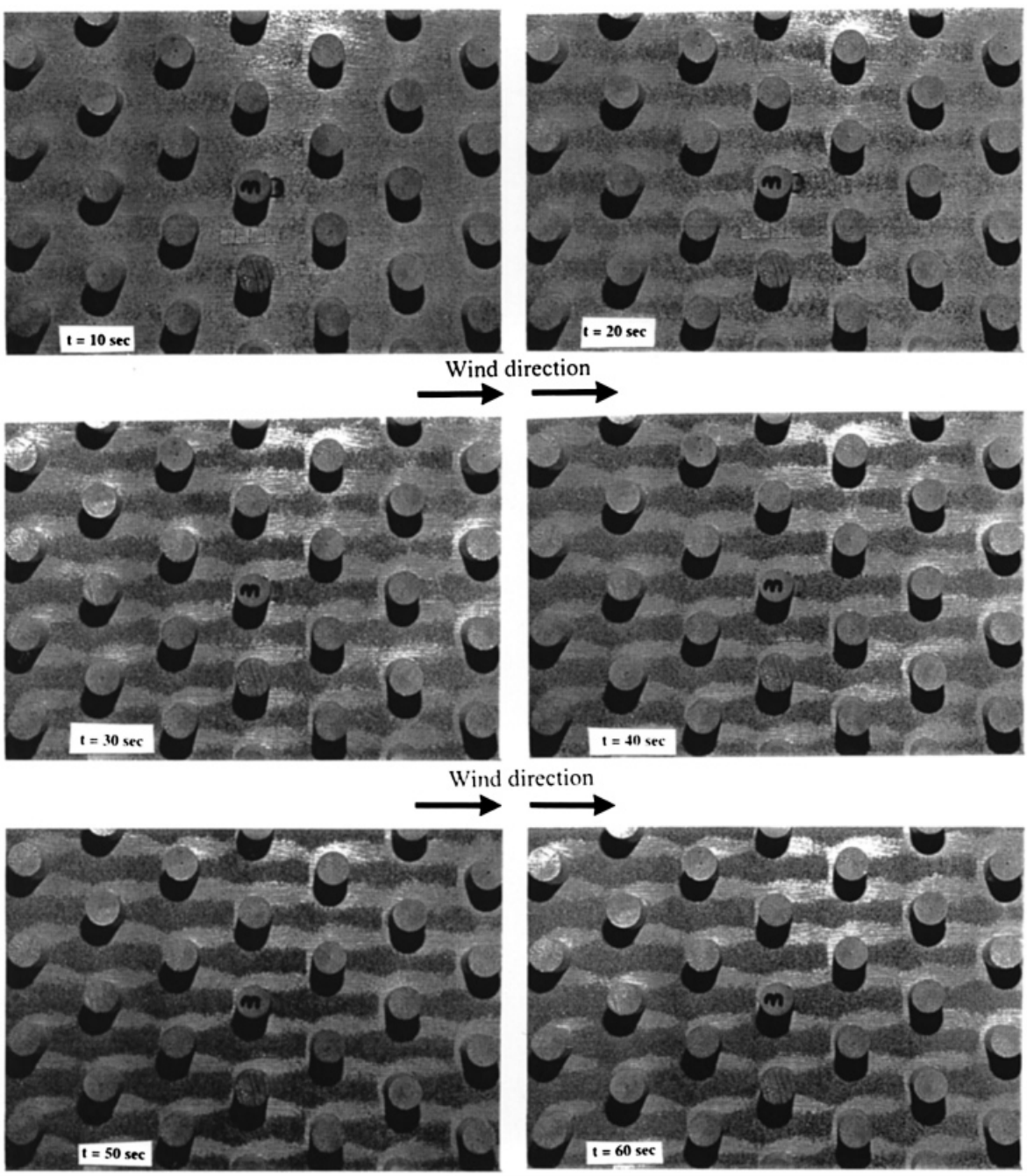

Figure 2. Lee-side sand deposit formation with time in experiment number A3-25T. The fully exposed cylinder at the beginning of each run caused an increased localized turbulence around and in the lee of each cylinder, resulting in sand deposition for two, principal reasons: (i) the formation of the wake zone behind the cylinder; and (ii) the promotion of entrainment of sand due to the sheltering effect

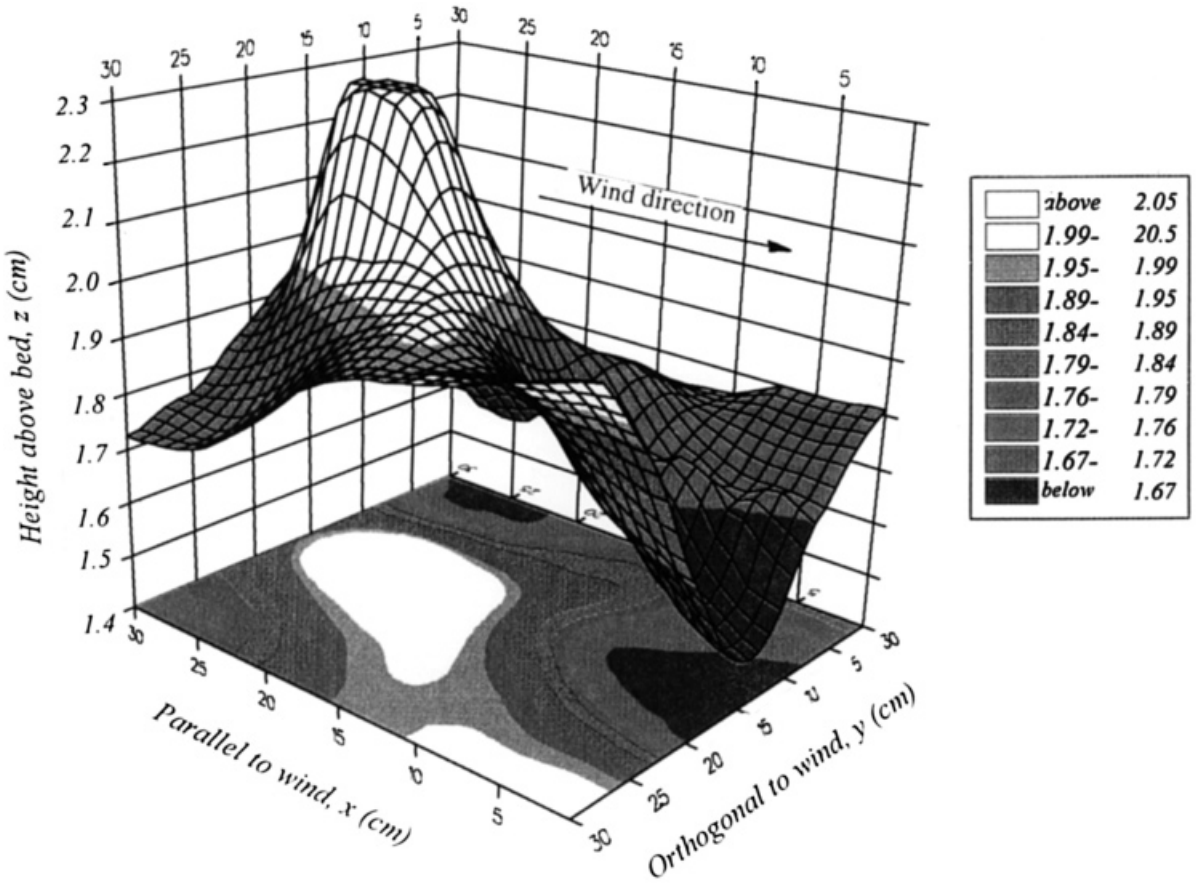

Figure 3. A typical sand deposition pattern around a central cylinder located at a distance of 20·0 cm from the upwind edge of the array in experiment number A1-40T. A concave surface of deposited sand was formed between adjacent completely buried cylinders

cylinders were buried. In particular, increased values of sand flux were recorded as the downwind cylinders of those observed began to be buried. This is attributed to: (i) the saltation path lengths of grains becoming longer than the remaining length of the test bed still not buried; and (ii) the change in the surface fixed roughness as the cylinders became buried, leading to an increase in the concentration of saltating grains due to diminished interference between the grains and the array elements.

The rate of change of sand flux

The experiments have shown that arrangements of cylindrical elements significantly curtail sand movement. Figure 5 shows that escaping sand flux in arrays A2, A3 and A4 increased at a low rate for a short period of time and then at a relatively higher rate until the end of the experiment. The increase in sand flux is expected to be maintained until an equilibrium sand transport rate is achieved (equal to the equilibrium upwind sand transport rate). This confirms that as the array fills up, it loses effectiveness as a trap for aeolian sand. In experiments with arrays A1 and A2 (widely spaced cylinders) and the lower shear velocity, the accumulation rate was slow and fluctuating. The duration of experiments with arrays A1 and A2 was too short to submerge the cylinders and therefore the process is revealed most clearly in the case of array A3. Figure 5 indicates that the rate of change of the escaping flux depends upon both upstream wind speed and the characteristics of the test bed.

An initial proportional transport rate reduction has been calculated by dividing the average sand transport rate during the first 600 s of the total time period in the presence of the array, by the associated equilibrium sand flux measured under similar conditions but in the absence of the array. The initial proportional sand

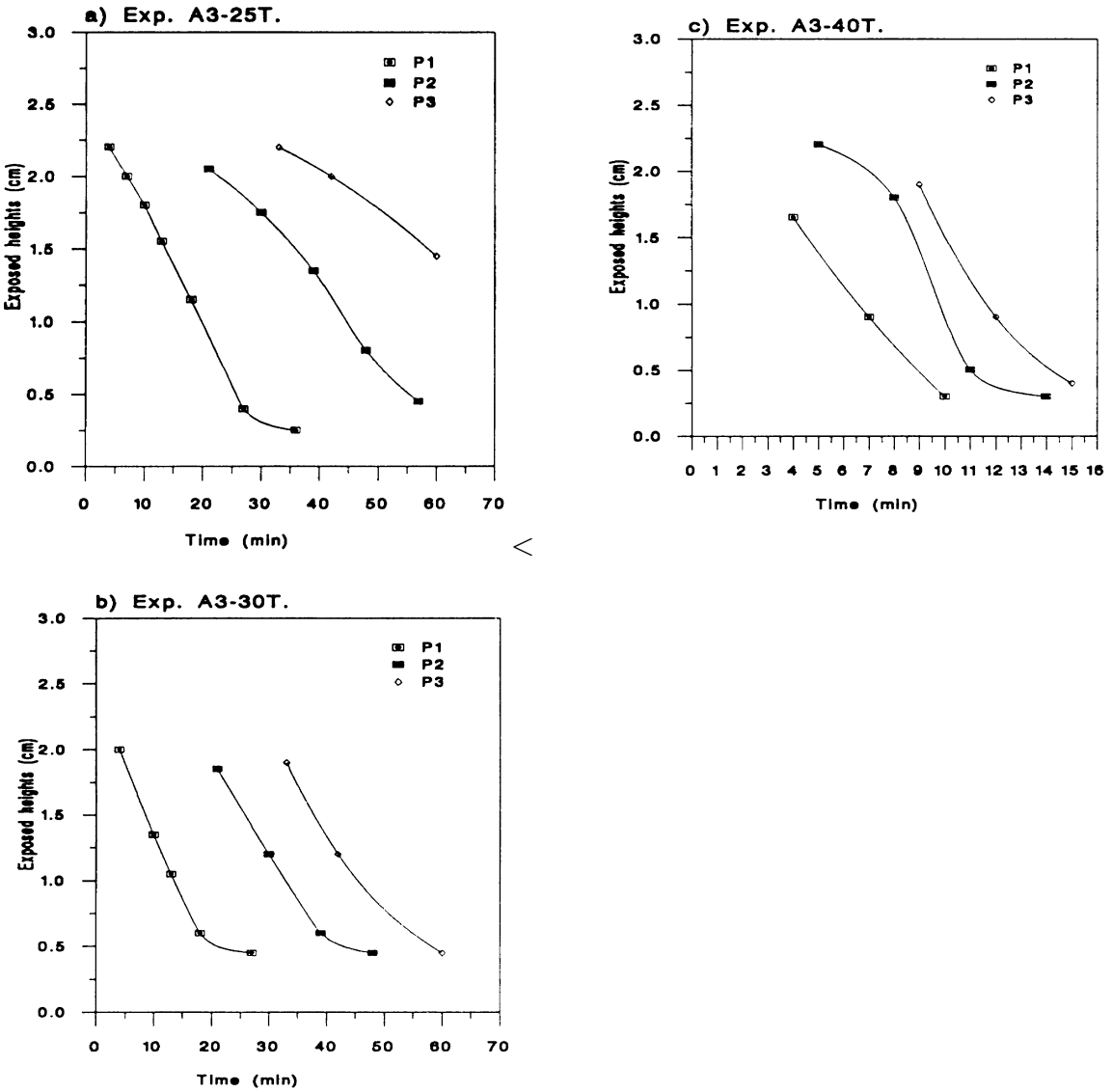

Figure 4. Change of exposed cylinder heights with time in array A3. The three positions of measurements are P1 = 39·8 cm, P2 = 119·4 cm and P3 = 199 cm downwind from the first row of cylinders. The rate of burial is a function of the position of the cylinder in the array

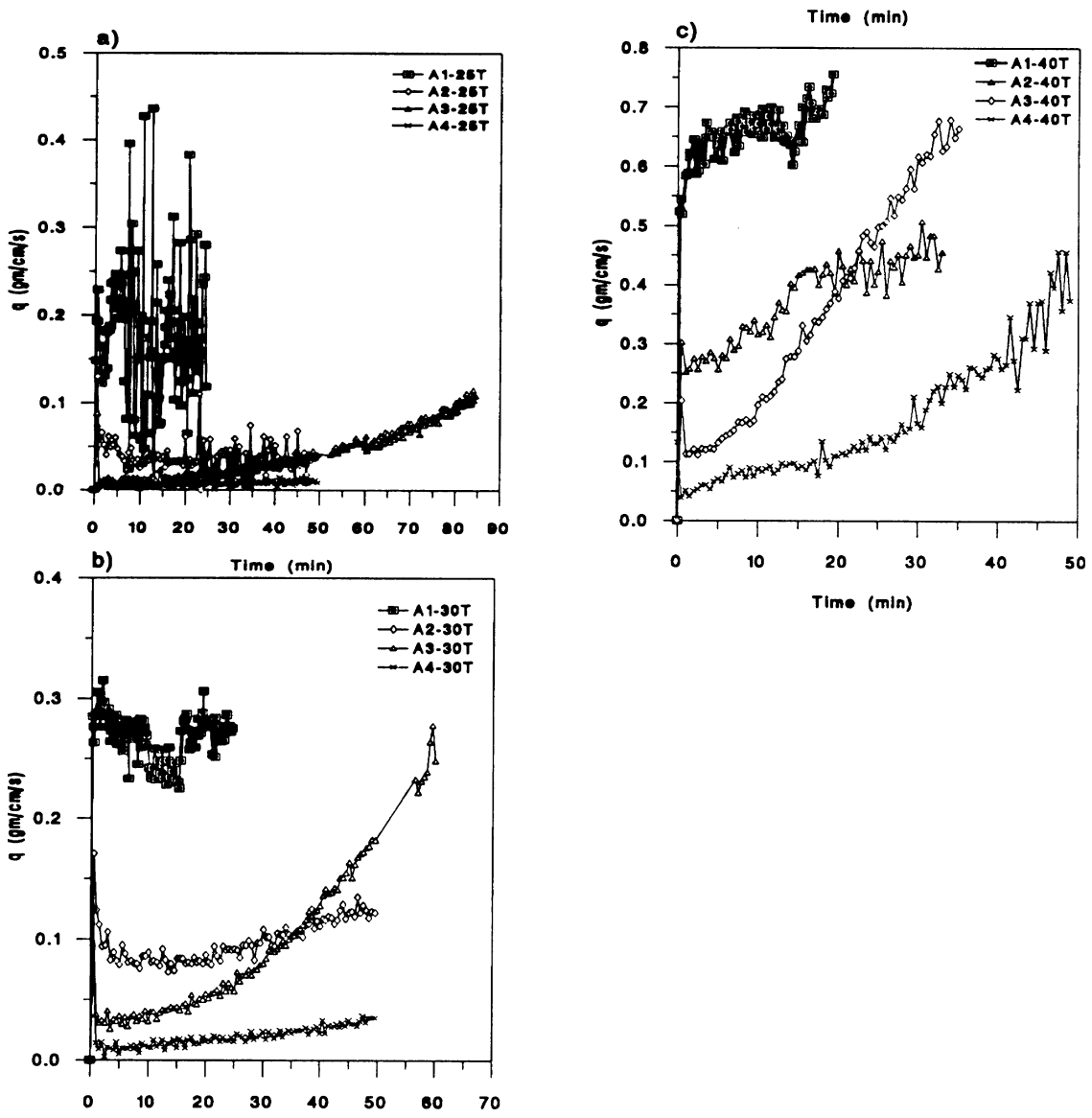

Figure 5. Rates of escaping sand flux over the four test beds used in this study with time. See Table II for details of experiments

Table III. Summary of some factors affecting the rate of initial sand flux

Experiment no.	Ratio of sand pass zone to width of unit area*	Basal to frontal area ratio of cylinder	Ratio of intervening surface shear stress to total fluid shear†	Ratio of initial sand flux to equilibrium sand flux
A1-25T	0·6	0·785	0·118	0·86
A1-30T	0·6	0·785	0·118	0·827
A1-40T	0·6	0·785	0·118	0·88
A2-25T	0·6	0·392	0·062	0·223
A2-30T	0·6	0·392	0·062	0·276
A2-40T	0·6	0·392	0·062	0·42
A3-25T	0·2	0·785	0·036	0·066
A3-30T	0·2	0·785	0·036	0·1136
A3-40T	0·2	0·785	0·036	0·209
A4-25T	0·2	0·392	0·018	0·035
A4-30T	0·2	0·392	0·018	0·0423
A4-40T	0·2	0·392	0·018	0·1004

* Ratio between the width of unit area, perpendicular to the flow, minus cylinder diameter and same width.
† Calculated using shear stress partitioning theory demonstrated by Raupach (1992), i.e. $\tau_s/\tau = 1/(1 + \beta\lambda)$ where τ is the total shearing stress (with cylinders on the surface), τ_s is the shearing stress on the surface between the cylinders and β is the ratio of element to surface drag coefficients.

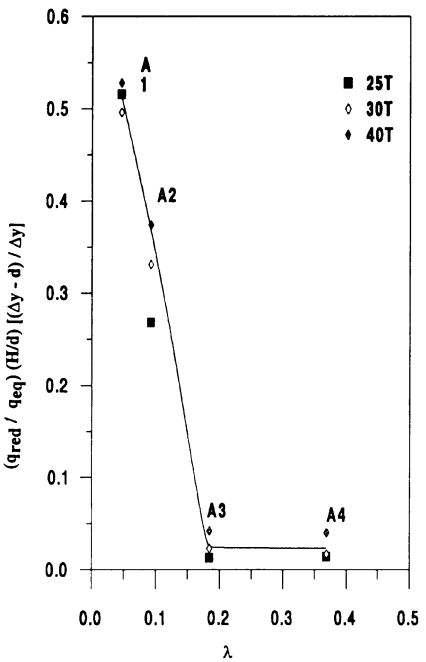

Figure 6. Non-dimensional relationship between initial reduction in sand flux and cylinder density (λ). This reduction has been calculated by dividing the average flux (q) during the first 10 min in the presence of the array, by the equilibrium flux (q_{eq}) under similar conditions in the absence of the array. d is the diameter of the cylinder, H is the height of the cylinder, Δy is the width of unit area associated with a cylinder, and λ is the concentration of non-erodible elements on the test bed given by (dH/ unit area)

transport rate due to the presence of different cylinder densities is shown in Table III, which also summarizes some factors affecting it. The data are replotted in Figure 6 in a dimensionless form that also reflects the array geometry. Figure 6 indicates that as the density of cylinders increased, the percentage reduction in sand flux increased, but the severest effect on the initial sand flux downwind of the array started at a test bed concentration of $\lambda \approx 0{\cdot}18$ and remained nearly unchanged with higher cylinder concentrations.

DISCUSSION

Laboratory and field tests by several researchers, such as Ash and Wasson (1983), Wasson and Nanninga (1986) and Buckley (1987), have shown that arrays of non-erodible elements significantly curtail sand movement. Measurement of sand flux over a short (250 cm) sand-free rough test bed placed in the path of sand transported over a flat bed at an equilibrium rate showed that initially the percentage of sand flux penetrating the 250 cm test bed length decreased with increasing array density. A relationship between the dimensions of the non-erodible element array and reduced sand flux (q_{red}) can be defined for the particular test bed length used in the reported experiments as:

$$q_{\mathrm{red}} = q_{\mathrm{eq}}(d/H)[\Delta y/(\Delta y - d)](0 \cdot 68 - 3 \cdot 5\lambda) \text{for} \quad \lambda \leq 0 \cdot 18 \tag{3}$$

$$q_{\mathrm{red}} = q_{\mathrm{eq}}(d/H)[\Delta y/(\Delta y - d)](0 \cdot 025) \qquad \text{for} \quad \lambda > 0 \cdot 18 \tag{4}$$

where q_{eq} is the equilibrium rate of sand transport arriving at the test bed, d is the diameter of the cylinder, H is the height of the cylinder, and Δy is the width of unit area associated with a cylinder and parallel to the flow direction. It should be noted that the equation is based on only four different arrays and therefore has unproven generality.

In this study, it was found that the sand flux over and through the test bed was gradually restored as the cylinders of the array were buried in deposited sand. The increase in the burial rate was sustained until an equilibrium sand transport rate was achieved, equal to the upstream sand flux (as observed clearly with the results for array A3). This increase is attributed to the reduction in the fixed surface roughness as the cylinders became buried, leading to a reduction in protected area; subsequently, the concentration of saltating grains increases and the saltation sequences are sustained. The increase of the escaping sand flux with time corresponds to a reduction in the deposition rate in the array.

At some critical concentration of non-erodible elements, the shear stress on the surface between them may fall everywhere to subthreshold values causing sand transport to cease. Marshall (1971) suggested that this value is reached when λ is equal to approximately 0·03, while Gillette and Stockton (1989) suggested a value of λ equal to 0·5. In the present study, it was noted that the sand flux did not reach zero over any of the test beds, even in experiments with a low wind speed and higher element concentration ($\lambda = 0{\cdot}369$). This endorses the view of Nickling and McKenna Neuman (1995) that the results of Gillette and Stockton (1989) are more consistent with observed sand activity than those of Marshall (1971).

Each fully exposed cylinder caused a local flow disturbance, including a lee-side wake that encouraged sand deposition. This was apparent from the formation of a lee-side deposit as soon as the sand started to blow. The form of this type of deposit is influenced by the element density of the array, the dimensions of each cylinder and the upstream wind speed. It also varied with the position of the cylinder in the array, particularly downwind distance. Although the wake zone characteristics behind an obstacle are known to be a function of the dimensions of the obstacle and the upwind speed, the flow patterns in the wake zone are not fully understood and become more complex if sand particles are present (Iversen *et al.*, 1991).

The experimental results show that the sand deposition and sand flux along an array consisting of regularly distributed cylinders are neither uniform nor steady. The results for the lower cylinder concentration (short cylinders and wide spacing) show that the cylinders in the first row started to be buried immediately after the start-up of the wind tunnel. This was followed by a gradual drifting of sand onto the downwind elements of the array. With a higher cylinder concentration, the situation is more complex, and the drifting started to occur at two positions, around the first row of cylinders and at a distance further downwind (nearly 50 to

75 cm from the upstream edge of the array). This observation indicates that the development length of the saltation layer plays a crucial role in the sand deposition process.

These experiments were limited to arrays of cylinders with heights and diameters of the same order as saltation dimensions. Interpretation of the findings with a view to practical application should pay due regard to this restriction. In many field applications, the non-erodible elements are disposed in a more or less random way and their heights may be variable. It has been claimed by Marshall (1971) that the total drag on randomly distributed elements remains fairly close to that found on regular patterns of identical elements. This, if sustained, would add some generality to the experimental results. The difficulty of scaling up (i.e. changing radically the ratio of saltation length to element size and spacing), however, has yet to be considered. The increase of scale can be expected to reduce the gradients of shear stress and transport rate in terms of saltation length units.

CONCLUSIONS

A number of conclusions may be drawn from this study.

1. An array of fixed cylinders, surface-mounted in the path of a sand-laden flow induces sand to deposit.
2. The pattern of deposition is related to changes in the boundary layer and is not uniform with distance downwind.
3. Deposition changes the degree of exposure of the cylinders, so the boundary layer (and consequently the deposition process) changes with time.
4. The experimental results confirm that the sand flux along an array consisting of regularly distributed cylinders is neither uniform nor steady, and that the development of an erodible deposited sand surface plays a crucial role in the restoration of sand flux along the rough surface.
5. In none of the main experiments, even those with a high element concentration and a low wind speed, did the sand flux over and between the non-erodible elements reach zero in the 2·5 m test bed. Transport was sustained in this length by the elastic collision of the moving sand grains with the hard element and tunnel floor surfaces. The elements were never completely buried because of the wind scouring associated with the development of eddies and vortices around each element.
6. As the total number of completely buried cylinders increased, the role of saltating grains in modifying the effective surface roughness became progressively more important compared with the role of the exposed height of non-erodible elements.
7. The characteristic form of the lee-side deposition varied with the element density of the array, the dimensions of the non-erodible elements, the free upstream wind and the distance downwind from the leading edge of the array.

ACKNOWLEDGEMENTS

The authors would like to express thanks to Mr Bill Lowson for his excellent technical assistance during the laboratory work.

REFERENCES

Al-Awadhi, J. M. and Willetts, B. B. 1998. 'Transient sand transport rates after wind tunnel start-up', *Earth Surface Processes and Landforms*, **22**, 21–30.

Al-Sudairawi, M. 1992. The Effect of non-erodible elements on sand transport rate, PhD thesis, University of Aberdeen, UK.

Antonia, R. A. and Luxton, R. E. 1971. 'The response of a turbulent boundary layer to a step change in surface roughness, Part 1. Smooth to rough', *Journal of Fluid Mechanics*, **48**, 721–761.

Arya, S. P. S. 1975. 'A drag partition theory for determining the large-scale roughness parameter and wind stress on the Arctic pack ice', *Journal of Geophysical Research*, **80**, 3447–3454.

Ash, J. E. and Wasson, R. H. 1983. 'Vegetation and sand mobility in the Australian desert dunefield', *Zeitchrift fur Geomorphologie*, Supplementum 45, 7–25.

Boundy, B. and Leach, R. 1990. The Effect of Surface Roughness on Threshold Velocity and Flux of 145 Micron Sand at Atmospheric and Martian Pressures, Informal Report, NASA Ames Research Center.
Bradley, E. F. 1968. 'A micrometeorological study of velocity profiles and surface drag in the region modified by a change in surface roughness', *Quarterly Journal of Royal Meteorological Society*, **94**, 361–379.
Buckley, R. 1987. 'The effect of sparse vegetation on the transport of dune sand by wind', *Nature*, **325**, 426–428.
Gillette, D. A. and Stockton, P. H. 1989. 'The effect of non-erodible particles on wind erosion at erodible surfaces', *Journal of Geophysical Research*, **94**, 12885–12893.
Iversen, J. D., Wang, W. P., Rasmussen, K. R., Mikkelsen, H. E. and Leach, R. N. 1991. 'Roughness element effect on local and universal saltation transport', *Acta Mechanica*, Supplementum 2, 65–75.
Jensen, N. O. 1978. 'Change of surface roughness and the planetary boundary layer', *Quarterly Journal of Royal Meteorological Society*, **104**, 351–356.
Logie, M. L. 1982. 'Influence of roughness elements and soil moisture on the resistance of sand to wind erosion', in Yaalon, D. H. (Ed.), *Aridic Soils and Geomorphic Processes, Catena*, Supplement 1, 161–173.
Lyles, L. 1977. 'Wind erosion: processes and effects on soil productivity', *Transactions, American Society of Agricultural Engineers*, **20**, 880–884.
Lyles, L. and Allison, B. E. 1975. 'Wind erosion: Uniformly spacing nonerodible elements eliminates effects of wind direction variability', *Journal of Soil and Water Conservation*, **30**, 225–226.
Lyles, L., Schrandt, R. L. and Schneidler, N. F. 1974. 'How aerodynamic roughness elements control sand movement', *Transactions, American Society Agricultural Engineers*, **17**, 134–139.
Marshall, J. K. 1971. 'Drag measurements in roughness arrays of varying density and distribution', *Agricultural Meteorology*, **8**, 269–292.
McKenna Neuman, C. and Nickling, W. G. 1995. 'Aeolian sediment flux: Non-linear behaviour on developing deflation lag surfaces', *Earth Surface Processes and Landforms*, **20**, 423–435.
Nickling, W. G. and McKenna Neuman, C. 1995. 'Development of deflation lag surface', *Sedimentology*, **42**, 403–414.
O'Loughlin, E. M. and Macdonald, E. G. 1964. 'Some roughness-concentration effects on boundary resistance', *La Houille Blanche*, **7**, 773–783.
Raupach, M. R. 1992. 'Drag and drag partition on rough surfaces', *Boundary-Layer Meteorology*, **60**, 375–395.
Schlichting, H. 1936. 'Experimentelle untersuchungen zum rauhigkeits problem', *Ing.-Arch*, **7**, 1–34 (English translation: NACA Technical Memo, No. 823 –1936).
Wasson, R. J. and Nanninga, P. M. 1986. 'Estimating wind transport of sand on vegetated surfaces', *Earth Surface Processes and Landforms*, **11**, 505–514.
Wooding, R. A., Bradley, E. F. and Marshall, J. K. 1973. 'Drag due to regular arrays of roughness elements of varying geometry', *Boundary-Layer Meteorology*, **5**, 285–308.

